Available online at www.sciencedirect.com
ScienceDirect
Journal of Power Sources 177 (2008) 211–216
JOURNAL OF POWER SOURCES
www.elsevier.com/locate/jpowsour

Short communication

The effect of tartrate on the morphological and structural characteristics of lead–tin electrodeposit from an alkaline bath

J.L.P. Siqueira, I.A. Carlos *

Departamento de Química, Universidade Federal de São Carlos, CP 676, 13565-905 São Carlos, SP, Brazil

Received 22 August 2007; received in revised form 8 November 2007; accepted 9 November 2007
Available online 19 November 2007

Abstract

The electrodeposition of Pb–Sn alloys from a tartrate-alkaline plating bath can lead to a deposition of pure lead or a normal codeposition of lead–tin depending on the deposition potential. The percentage of tin in the Pb–Sn deposit obtained at ∼−1.15 V increases from 4.08 wt.% to 20.7 wt.% as the charge density rises from 2.5 C cm^{-2} to 5.0 C cm^{-2} and then decreases from 12.07 wt.% to 7.52 wt.% as the charge density rises from 7.5 C cm^{-2} to 10.0 C cm^{-2}. SEM images show that the Pb and Pb–Sn deposits obtained from a tartrate-alkaline bath did not, in general, show dendritic growth.

X-ray analysis of the deposits obtained at −0.83 V with 5.0 C cm^{-2} or 10.0 C cm^{-2} indicated the presence of Pb and Pb_2PtO_4 and the absence of Sn. However, those obtained at −1.15 V and the same charge densities (q_d) showed the presence of Pb, Pb_2SnO_4, $PbSnO_3$ and $PtSn_4$. The Pb_2PtO_4 and $PtSn_4$ compounds were formed because the electrodeposition process occurred onto Pt substrate.

Keywords: Lead–tin; Electrodeposition; Tartrate-alkaline bath; X-ray spectroscopy; Morphology

1. Introduction

Lead–tin alloy electroplating has been achieved with a number of solutions: fluoborate, fluosilicate, sulfamate and alkaline sorbitol [1–3] and in the present study these deposits are prepared from an alkaline tartrate plating bath developed in this laboratory.

Previous studies indicate limits for the optimum concentration of tin in the alloy for application in the grid of a lead battery, which should be high enough to prevent the formation of an insulating PbO phase at the grid surface, but low enough to avoid hindrance of PbO_2 formation [4].

In earlier work [3], we found the Sn content in Pb–Sn alloy deposited from alkaline sorbitol electrolyte, at −1.17 V, to be 19 wt.% at 5.0 C cm^{-2} or 25.6 wt.% at 10.0 C cm^{-2}. It was therefore concluded that these films were probably unsuitable for lead–acid batteries.

In this paper, we report a study of lead–tin deposition onto a platinum electrode in an alkaline tartrate plating bath, using cyclic voltammetry. The influence of charge density (q_d) and deposition potential (E_d) on the morphology and structure of the lead–tin deposit was investigated by scanning electron microscopy and on the composition by energy-dispersive X-ray spectroscopy. Moreover, the composition of the crystalline phases of the lead–tin deposit was investigated by X-ray diffraction.

2. Experimental

All chemicals were analytical grade. Double-distilled water was used throughout. Each electrochemical experiment was performed in a freshly prepared alkaline bath, containing 0.05 M $Pb(NO_3)_2$ and/or 0.05 M $SnCl_2$, 0.4 M NaOH and 0.1 M tartrate. In this plating bath, plumbite and stannite anions were stabilized by tartrate anions, since in its absence, at this NaOH concentration 0.4 M NaOH PbO and SnO_2 were precipitated [5,6]. A Pt disk (0.196 cm^2), a Pt plate and an Hg/HgO/NaOH (1.0 M) electrode with an appropriate Luggin capillary were employed as working, auxiliary and reference electrodes, respectively. Immediately prior to the electrochemical measurements, the Pt working electrode was ground with 0.3 μm alumina, immersed in concentrated sulphuric–nitric

* Corresponding author. Tel.: +55 16 33518067; fax: +55 16 33518350.
E-mail address: diac@power.ufscar.br (I.A. Carlos).

0378-7753/$ – see front matter © 2007 Elsevier B.V. All rights reserved.
doi:10.1016/j.jpowsour.2007.11.027

acid solution and then rinsed with deionized water. Potentiodynamic curves were recorded with a PAR electrochemical system based on an EG&G-PAR 173 potentiostat/galvanostat, at a scanning rate of 10 mV s^{-1}. All experiments were carried out at room temperature (25 °C). Potentiostatic deposits were produced with charge densities of 2.5 C cm^{-2}, 5.0 C cm^{-2}, 7.5 C cm^{-2} and 10.0 C cm^{-2}. Deposition charges were measured with an EG&G-PAR 379 coulometer.

The XRD samples of Pb–Sn deposits were prepared chronopotentiometrically at deposition potentials of −0.83 V and −1.15 V, with q_d = 5.0 C cm^{-2} and 10.0 C cm^{-2} at each E_d. Thus, the X-ray diffraction patterns were produced with filtered Cu Kα radiation (1.54051 Å), using a Rigaku Rotaflex RU 200B rotating-anode X-ray goniometer. The diffraction experiments were done in a 2θ scan mode (grazing incidence type, with ω fixed at 2°).

Scanning electron microscopy (SEM) photographs were taken with a Philips XL 30-FEG. Energy-dispersive X-ray spectroscopy (EDS) was performed with an Oxford ELX; Si(Li) detector with ultrathin Be window.

3. Results and discussion

3.1. Voltammetric experiments

Fig. 1(a) shows voltammograms recorded from the Pt substrate, with the Pb salt alone (broken line) or both Pb and Sn salts (solid line) in the plating solution. The initial potential was −0.5 V, the sweep reversal potential was −1.6 V and final potential was 0.4 V. The main features of the Pb–Sn voltammogram (solid line) are two cathodic peaks c_1 (peak potential, $E_p \sim -0.83$ V) and c_2 ($E_p \sim -1.15$ V). The increase in the current density (j) at potentials more negative than −1.35 V is due to the H_2 evolution reaction (HER). The anodic sweep shows three anodic processes: peaks a_1 ($E_p \sim -0.92$ V), a_2 ($E_p \sim -0.74$ V) and a_3 ($E_p \sim -0.52$ V).

The Pb deposition (broken line) begins at ∼−0.75 V, with a steep increase in the current density. After the cathodic peak ($E_p \sim -0.78$ V), j decreases, reaching a diffusion-limited current density plateau at ∼5 mA cm^{-2}. Beyond ∼−1.30 V the current density increases sharply, due to the HER.

The peak c_1 ($E_p \sim -0.83$ V, solid line) in the Pb–Sn voltammogram appears at a potential close to that of pure lead deposition ($E_p \sim -0.78$ V) and can thus be associated with Pb deposition (see Sections 3.2 and 3.4).

The lead dissolution process on Pt substrate (Fig. 1(a), broken line) shows three anodic peaks (∼−0.63 V; ∼−0.50 V; ∼−0.35 V) and a shoulder (∼−0.52 V), which correspond to lead passivation, as can be seen better in Fig. 1(b). This figure shows the voltammetric curve for a Pb electrode in 0.4 M NaOH + 0.1 M tartrate. Two anodic peaks are seen at ∼−0.52 V and ∼−0.41 V.

Voltammograms recorded for the Pt substrate, using only the Sn salt (broken line) or both Pb and Sn salts (solid line) in the plating solutions, are presented in Fig. 2(a). The initial potential was −0.5 V, the sweep reversal potential was −1.6 V and final potential was 0.4 V. Comparing the tin alone (broken

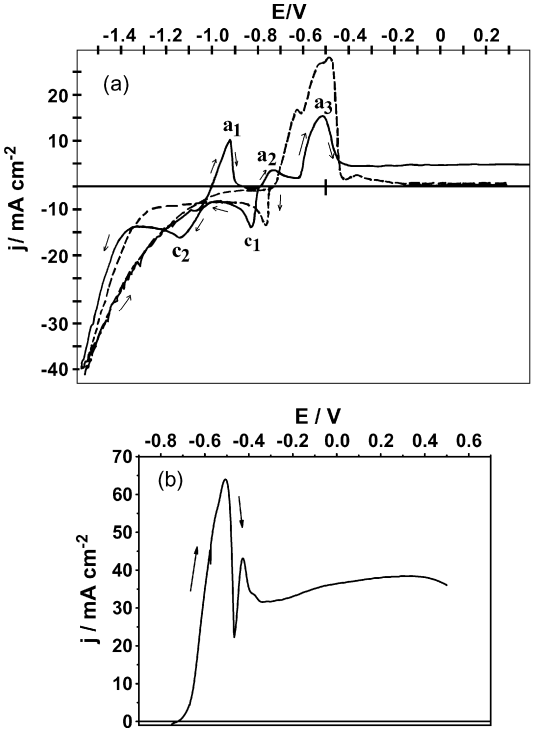

Fig. 1. Voltammetric curves for platinum substrate (a) in 0.050 M $Pb(NO_3)_2$ + 0.050 M $SnCl_2$ + 0.10 M $NaKC_4H_4O_6$ + 0.40 M NaOH (—) and 0.050 M $Pb(NO_3)_2$ 0.10 M $NaKC_4H_4O_6$ + 0.40 M NaOH (- - - -), initial potential: −0.5 V; sweep reversal potential: −1.6 V; final potential: 0.4 V and (b) anodic scan for Pb electrode in 0.10 M $NaKC_4H_4O_6$ + 0.40 M NaOH; v = 10 mV s^{-1}.

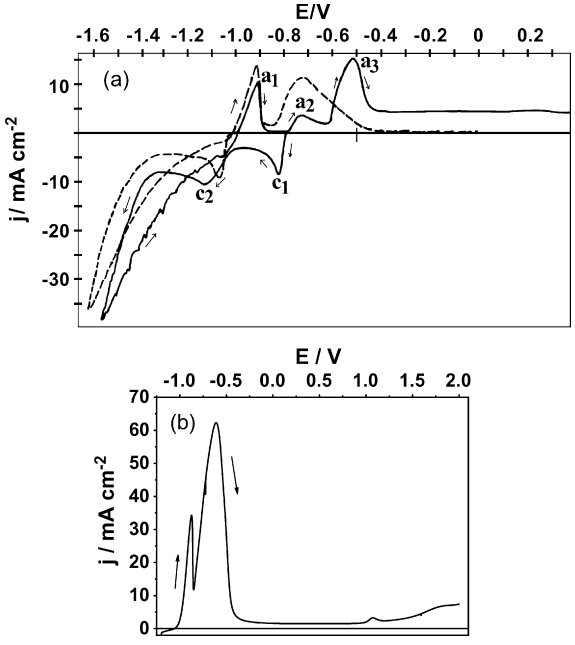

Fig. 2. Voltammetric curves for platinum substrate (a) in 0.050 M $Pb(NO_3)_2$ + 0.050 M $SnCl_2$ + 0.1 M $NaKC_4H_4O_6$ + 0.4 M NaOH (—) and 0.050 M $SnCl_2$ + 0.1 M $NaKC_4H_4O_6$ + 0.4 M NaOH (- - - -), initial potential: −0.5 V; sweep reversal potential: −1.6 V; final potential: 0.4 V and (b) anodic scan for Sn electrode in 0.1 M $NaKC_4H_4O_6$ + 0.4 M NaOH; v = 10 mV s^{-1}.

line) and Pb–Sn potentiodynamic curves (solid line), peak c_2 (∼−1.15 V) can be associated with Pb and Sn codeposition (see Sections 3.1 and 3.3). In the anodic voltammogram, two peaks for Sn passivation/dissolution (∼−0.91 V and ∼−0.72 V) are seen, which corroborating the results in Fig. 2(b). This figure shows the voltammetric curve for a tin electrode in 0.4 M NaOH + 0.1 M tartrate. Two anodic peaks can be seen at ∼−0.88 V and ∼−0.61 V.

Analyzing the Pb–Sn dissolution processes (solid line, Fig. 2(a)), the peak a_1 (E_p ∼ −0.92 V) probably corresponds to Sn dissolution/passivation and the peaks a_2 (E_p ∼ −0.74 V) and a_3 (E_p ∼ −0.52 V), respectively to Sn and Pb dissolution/passivation.

The authors have reported [3] that the difference between the Pb deposition potential ($E_{Pb^{2+}/Pb} = -0.80$ V) and the Sn deposition potential ($E_{Sn^{2+}/Sn} = -1.0$ V) from an alkaline sorbitol bath versus Hg/HgO/1 M NaOH reference electrode was 0.2 V. In the present study, the difference between $E_{Pb^{2+}/Pb}$ (−0.75 V) and $E_{Sn^{2+}/Sn}$ (−1.03 V, cathodic peak in Fig. 2(a), dotted line) versus Hg/HgO/1 M NaOH reference electrode was 0.28 V.

Comparing these systems, it can be inferred that sorbitol added to the bath draws together the deposition potential of the individual metals more than tartrate additive. Also, the authors observed two cathodic and four anodic peaks during voltammetric electrodeposition of Pb–Sn on a platinum substrate, from an alkaline sorbitol bath containing 0.05 M Pb^{2+} and 0.05 M Sn^{2+}. The potential of the first anodic peak, during the anodic sweep, was shifted to a more negative potential than the peaks observed with separate of Pb and Sn metals, demonstrating the physical energy of dispersion of Pb and Sn metals into grains in the Pb–Sn deposits on Pt substrate. However, in the present work, this shift was not observed, leading us to conclude that Pb and Sn are deposited independently of each other.

To characterize better the Pb–Sn reduction process, the reverse-scan voltammetric technique was used. The initial potential was −0.5 V and the sweep was reversed at several potentials: −0.85 V (Fig. 3(a)), −1.15 V (Fig. 3(b)) and −1.3 V (Fig. 3(c)). When the cathodic sweep was reversed at a potential of −0.85 V, an increase in the cathodic current density was seen, suggesting that Pb–Sn deposition occurs by nucleation [7]. With a limit potential of −1.15 V, a current plateau was observed, indicating that the plating process was under diffusion control [8]. When the sweep was reversal at ∼−1.3 V, the peak a_1 appears in the anodic scan which corresponds to Sn dissolution. Finally, when the sweep was reversed at −1.60 V (Fig. 1(a)), the current increased, probably indicating an increase in the area of Pb–Sn deposit.

Fig. 4(a) shows the Pb–Sn deposition voltammograms, at different sweep rates (v). It can be observed that the current density of the first peak increases as the sweep rate increases, suggesting that the deposition process is controlled by mass transport. The peak current of reduction of Pb^{2+} species is described by Eq. (1), which includes the reduction of soluble species to form insoluble species [9,10]

$$j_p = 367 n^{3/2} A C_0 D^{1/2} v^{1/2} \quad (1)$$

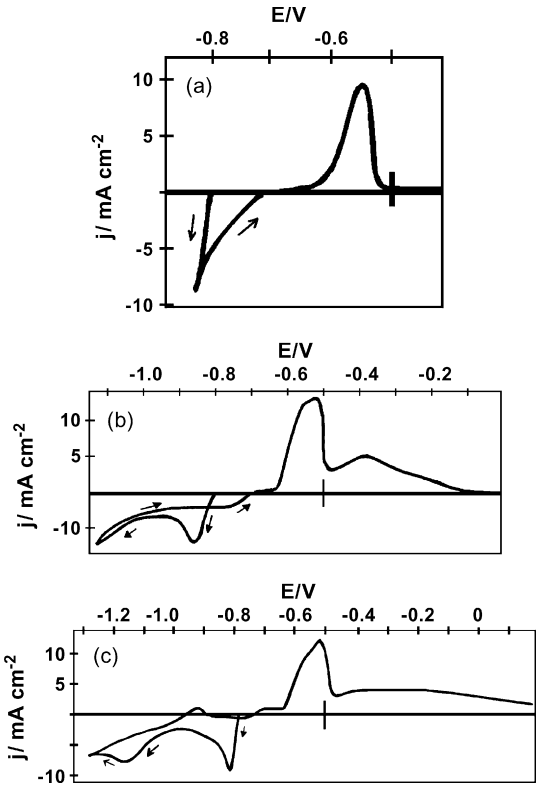

Fig. 3. Voltammetric curves for platinum substrate in 0.050 M $Pb(NO_3)_2$ + 0.050 M $SnCl_2$ + 0.10 M $NaKC_4H_4O_6$ + 0.40 M NaOH; initial potential: −0.5 V; effect of the limit potentials: (a) −0.85 V, (b) −1.15 V and (c) −1.30 V. $v = 10$ mV s^{-1}.

where n is number of electron; A is electrode area in cm^2; C_0 is concentration of electroactive species in mol L^{-1}; D is diffusion coefficient in cm^2 s^{-1}; v is rate of voltage scan in V s^{-1}.

Fig. 4(b) shows that the current density (j_p) of peak c_1 increases non-linearly with $v^{1/2}$. This result suggests that the Pb electrodeposition process is quasi-reversible in the region. Moreover, these results show that the HER was polarized with increase in the sweep rate from ∼−1.4 V ($v = 10$ mV s^{-1}) to ∼−1.1 V ($v = 200$ mV s^{-1}).

3.2. EDS analysis of the Pb–Sn deposits

Analyses by EDS were carried out (Table 1) in the region of peaks c_1 and c_2. Table 1 shows that Sn was not present in

Table 1
Energy-dispersive X-ray spectroscopy for electrodeposited films obtained chronoamperometrically

E_p (V)	q_d (C cm^{-2})	Pb (wt.%)	Sn (wt.%)
−0.83	5	100.00	0.0
−0.83	10	100.00	0.0
−1.15	2.5	95.92	4.08
−1.15	5	79.30	20.70
−1.15	7.5	87.92	12.07
−1.15	10	92.48	7.52

E_p: peak potential and q_d: charge density of deposit.

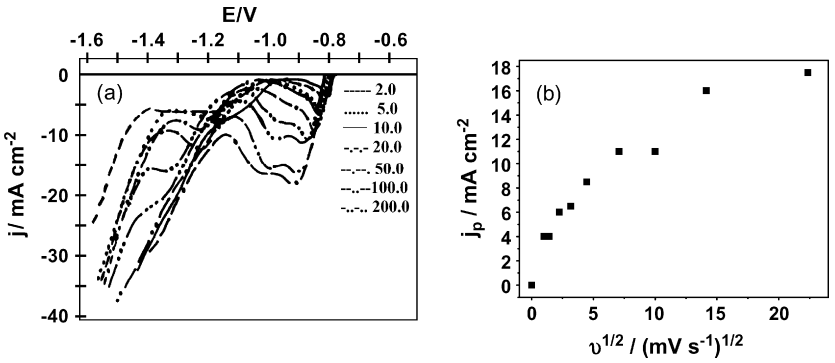

Fig. 4. (a) Voltammetric deposition curves for platinum substrate in 0.050 M $Pb(NO_3)_2$ + 0.050 M $SnCl_2$ + 0.1 M $NaKC_4H_4O_6$ + 0.4 M NaOH; at various sweep rates (v (mV s^{-1})): (- - - - -) 2.0; (· · ·) 5.0; (—) 10; (- · -) 20; (- - - - -) 50; (- - - - - -) 100; (- · · ·) 200. (b) Variation of j_p with $v^{1/2}$ for the current densities of the first voltammetric peak.

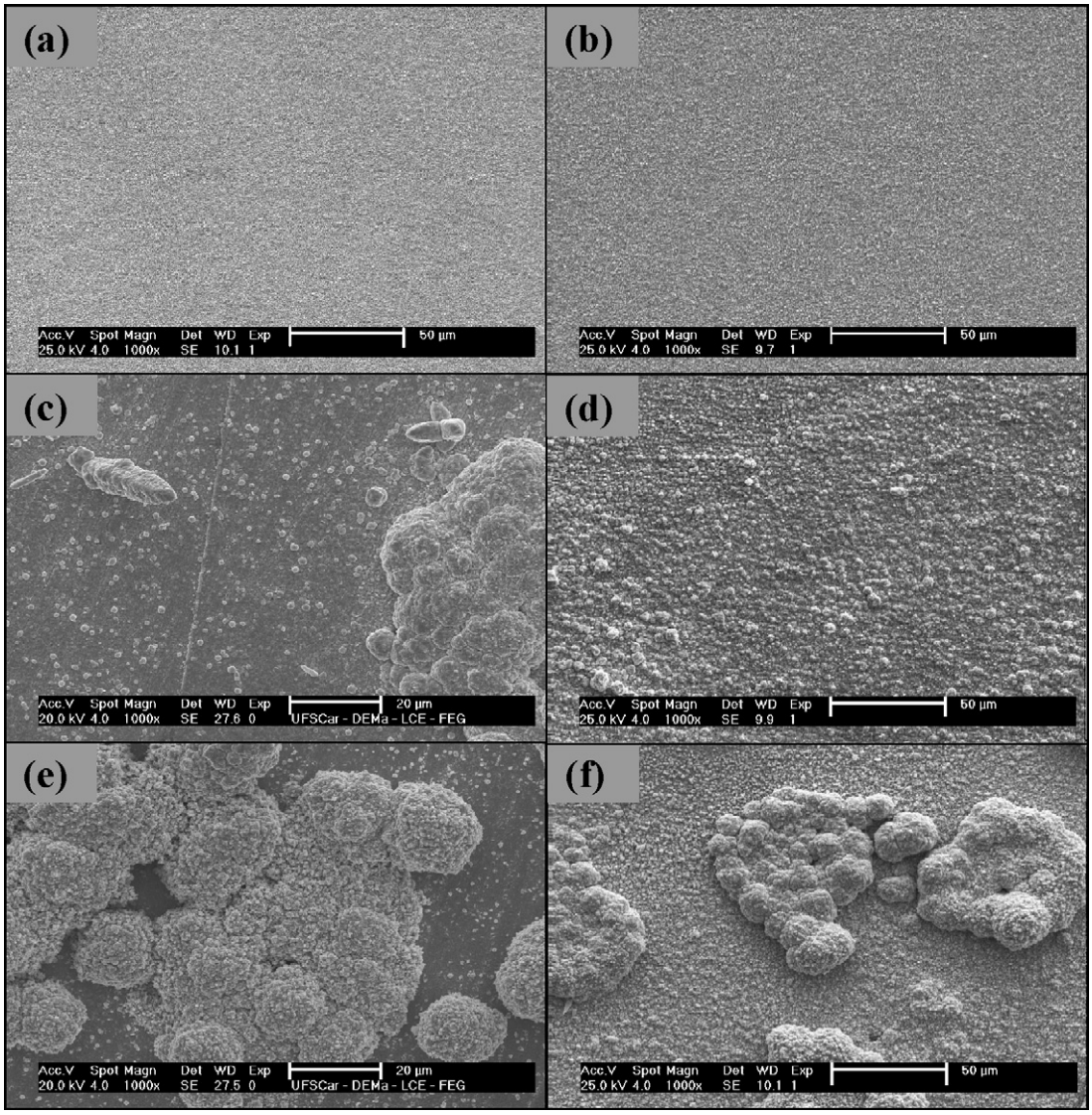

Fig. 5. SEM micrographs of Pb–Sn films obtained chronoamperometrically from −0.50 V to −0.83 V, with q_d at (a) 5.0 C cm^{-2} and (b) 10 C cm^{-2}, and from −0.50 V to −1.15 V, with q_d at (c) 2.5 C cm^{-2}, (d) 5.0 C cm^{-2}, (e) 7.5 C cm^{-2} and (f) 10 C cm^{-2}. Deposition solution: 0.050 M $Pb(NO_3)_2$ + 0.050 M $SnCl_2$ + 0.1 M $NaKC_4H_4O_6$ + 0.40 M NaOH.

the deposits obtained at a deposition potential (E_d) of −0.83 V, with $q_d = 5.0\,C\,cm^{-2}$ or $10.0\,C\,cm^{-2}$, while both Pb and Sn were found at −1.15 V, with q_d in the range from $2.5\,C\,cm^{-2}$ to $10.0\,C\,cm^{-2}$.

It can be seen in Table 1 that the percentage of Sn in the Pb–Sn deposit obtained at ∼−1.15 V increases from 4.08 wt.% to 20.7 wt.% as the charge density increases from $2.5\,C\,cm^{-2}$ to $5.0\,C\,cm^{-2}$ and then decreases to 12.07 wt.% and 7.52 wt.%, for $7.5\,C\,cm^{-2}$ and $10.0\,C\,cm^{-2}$, respectively.

Therefore, the composition of deposits obtained at −1.15 V depends on the amount deposited. Lead is dominant in the layer obtained at either potential.

The solid solubilities of tin in lead in the electrodeposited Pb–Sn layer obtained here at −1.15 V (Table 1) from the alkaline tartrate bath were in general lower than the equilibrium value of 19 wt.% Sn reported for thermal alloys [11]. Also, the content of Sn in the Pb–Sn deposit obtained at −1.15 V and $2.5\,C\,cm^{-2}$ was lower than those reported in electrodeposited alloys (∼6.8 wt.% Sn) [12,3], while that at a charge density of $10\,C\,cm^{-2}$ was similar [3].

The Pb–Sn deposits obtained at −1.15 V with $q_d = 2.5\,C\,cm^{-2}$ (4.08 wt.% Sn), $7.5\,C\,cm^{-2}$ (12.07 wt.% Sn) and $10.0\,C\,cm^{-2}$ (7.52 wt.% Sn) contain lower Sn content than those obtained from alkaline sorbitol baths [3]. This is due probably to that sorbitol and tartrate additives influence differently the Pb–Sn nucleation process.

3.3. Scanning electronic microscopy

SEM analysis was carried out on the Pb–Sn deposits formed from the alkaline tartrate solution of Pb and Sn salts, at −0.83 V, with $q_d = 5\,C\,cm^{-2}$ and $10.0\,C\,cm^{-2}$ (Fig. 5(a) and (b), respectively), and at −1.15 V, with $q_d = 2.5\,C\,cm^{-2}$, $5.0\,C\,cm^{-2}$, $7.5\,C\,cm^{-2}$ and $10.0\,C\,cm^{-2}$ (Fig. 5(c)–(f), respectively). Comparing these micrographs, it can be seen that the Pb deposits obtained at −0.83 V with $5.0\,C\,cm^{-2}$ and $10.0\,C\,cm^{-2}$ were uniformly smooth. However, it may be noted that at −1.15 V and $q_d = 2.5\,C\,cm^{-2}$, $7.5\,C\,cm^{-2}$ and $10.0\,C\,cm^{-2}$, irregular crystallites and clusters of irregular crystallites completely cover the substrate, while at $5.0\,C\,cm^{-2}$ there is a uniform and compact deposit of irregular crystallites. The latter result implies that the high Sn content (20.70 wt.% Sn) in the $5.0\,C\,cm^{-2}$ deposit, relative to those obtained at other q_d ($2.5\,C\,cm^{-2}$, $7.5\,C\,cm^{-2}$ and $10.0\,C\,cm^{-2}$), leads to a uniform and compact Pb–Sn deposit.

Micrographs of Pb–Sn films obtained from an alkaline sorbitol plating bath showed that when Sn was present in the layer, dendritic growth of the deposit was hindered [3]. However, it should be noted that in Pb–Sn deposits obtained from the alka-

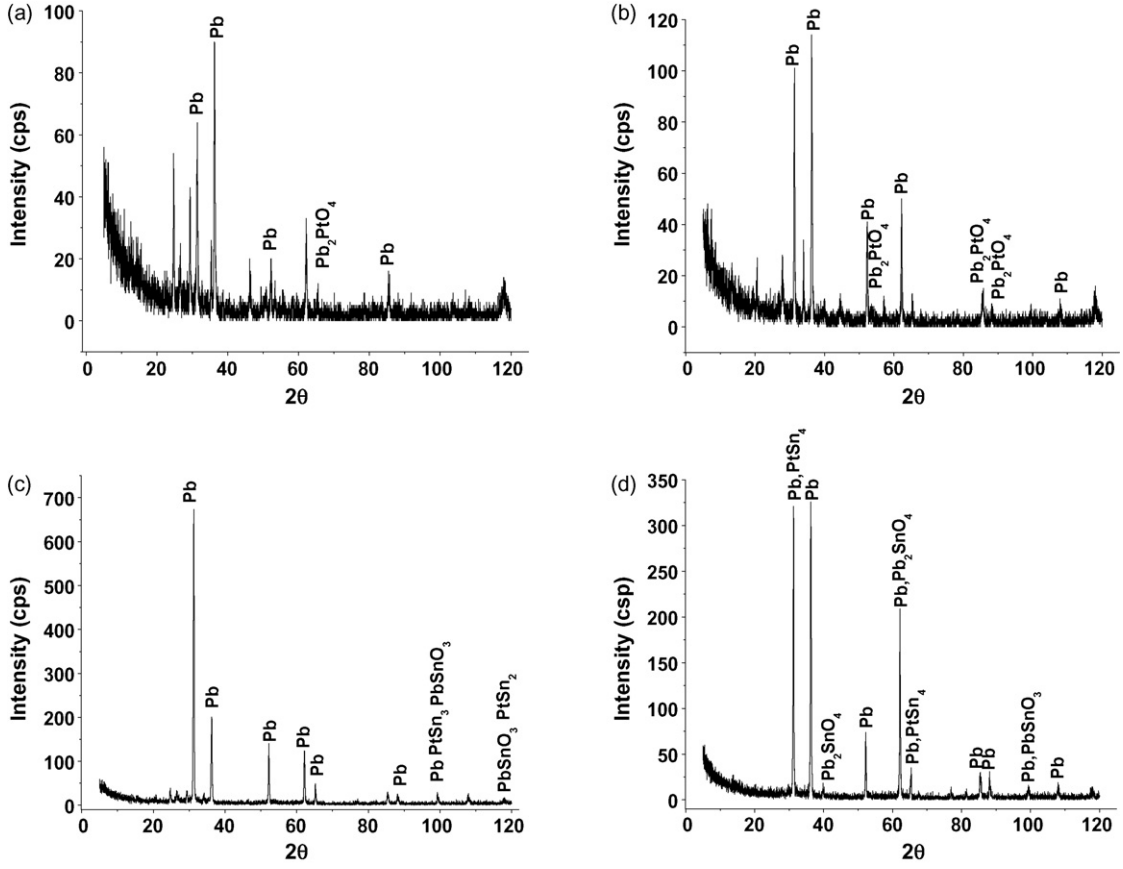

Fig. 6. X-ray diffraction patterns of deposits obtained chronoamperometrically from −0.50 V to −0.83 V ((a) and (b)) and −0.50 V to 1.15 V ((c) and (d)), with charge density of $5.0\,C\,cm^{-2}$ ((a) and (c)) and $10.0\,C\,cm^{-2}$ ((b) and (d)). Deposition solution: 0.050 M $Pb(NO_3)_2$ + 0.050 M $SnCl_2$ + 0.10 M $NaKC_4H_4O_6$ + 0.40 M NaOH. Pb(JCPDS-04-0686); Pb_2PtO_4(JCPDS-84-1257); $PtSn_4$(JCPDS-04-0744); $PbSnO_3$(JCPDS-17-0607).

line tartrate bath, only at −1.15 V and $q_d = 2.5\,C\,cm^{-2}$ were any dendrite crystallites observed, while at other E_d and q_d they were absent.

3.4. X-ray analysis of the Pb–Sn deposits

Fig. 6(a)–(d) show X-ray diffraction patterns of deposits obtained from a solution of Pb and Sn salts at −0.83 V and −1.15 V, with $q_d = 5.0\,C\,cm^{-2}$ and $10.0\,C\,cm^{-2}$ at each E_d.

The diffractograms from the deposits obtained at −0.83 V with $q_d = 5.0\,C\,cm^{-2}$ (Fig. 6(a)) or $q_d = 10.0\,C\,cm^{-2}$ (Fig. 6(b)) indicated the presence of Pb and Pb_2PtO_4 and the absence of Sn [15]. However, those obtained at −1.15 V, with $q_d = 5.0\,C\,cm^{-2}$ (Fig. 6(c)) or $q_d = 10.0\,C\,cm^{-2}$ (Fig. 6(d)), showed some peaks that could be attributed to Pb, $PbSnO_3$, Pb_2SnO_4 and $PtSn_4$ [13].

These results are consistent with the EDS (Section 3.2) finding that Sn was not deposited at −0.83 V.

The Pb_2PtO_4 and $PtSn_4$ compounds were formed since the electrodeposition process occurred on the platinum substrate.

Comparing the deposit obtained at −1.15 V with the one produced in similar potential conditions (−1.17 V) in an alkaline sorbitol Pb–Sn plating bath [3], it can be stated that the β-Sn detected in the Pb–Sn film deposited in the sorbitol bath was not present in the deposit obtained here in the alkaline tartrate Pb–Sn bath.

Petersson and Ahlberg [4,14,15] report that when the amount of tin in the Pb–Sn film was higher than 12 wt.%, the amount of PbO_2 formed decreases and the overpotential of oxygen evolution rises.

Although the content of Sn in these PbSn deposits are lower than 12 wt.% – at −1.15 V it was 4.08 wt.% ($2.5\,C\,cm^{-2}$), 12.07 wt.% ($7.5\,C\,cm^{-2}$) and 7.52 wt.% ($10.0\,C\,cm^{-2}$) they could cause problems in a trial to use the deposit in lead acid batteries due to the presence of oxides $PbSnO_3$ and Pb_2SnO_4.

4. Conclusions

1. Two cathodic peaks are observed during the potentiodynamic electrodeposition of lead–tin from an alkaline tartrate plating bath, with a potential difference of about 0.32 V. It is probable that the first cathodic peak is related to the deposition of lead and second to codeposition of Pb–Sn.
2. The deposition voltammetric curves at various sweep rates suggest that Pb–Sn deposition is controlled by mass transport.
3. The relationship between j_p and $v^{1/2}$ indicates that the Pb electrodeposition process is quasi-reversible.
4. EDS analyses show the occurrence of only Pb in the deposits obtained at the first peak and Pb–Sn in those at the second peak. The Sn content in the deposit depends on the total amount deposited.
5. The codeposition of Sn and Pb is normal because Pb is dominant in the deposit obtained at the more negative potential (−1.15 V).
6. SEM analyses showed that deposits obtained at −1.15 V and $q_d = 2.5\,C\,cm^{-2}$, $7.5\,C\,cm^{-2}$ and $10.0\,C\,cm^{-2}$ were formed of irregular crystallites and clusters of irregular crystallites completely covering the substrate, while at $5.0\,C\,cm^{-2}$ a uniform and compact deposit was formed of irregular crystallites.
7. The high Sn content in the $5.0\,C\,cm^{-2}$ Pb–Sn deposit leads to uniform and compact morphology.
8. X-ray analyses indicated the presence of Pb and Pb_2PtO_4 in the deposit formed at the first peak and Pb, Pb_2SnO_4, $PbSnO_3$ and $PtSn_4$ in that formed at the second (more negative) peak.
9. The Pb_2PtO_4 and $PtSn_4$ compounds were formed since the electrodeposition process occurred on the platinum substrate.

Acknowledgements

Financial support from the Brazilian research foundations: CNPq and FAPESP (Proc. No 04/14142-2) are gratefully acknowledged.

References

[1] A. Brenner, Electrodeposition of Alloys: Principles and Practice, vol. 1, Academic Press, New York, 1963.
[2] E.J. Roehl, Iron Ace 173 (1954) 140.
[3] J.L.P. Siqueira, I.A. Carlos, J. Power Sources 169 (2007) 361.
[4] I. Petersson, E. Ahlberg, J. Power Sources 91 (2000) 143.
[5] I.A. Carlos, J.L.P. Siqueira, G.A. Finazzi, M.R.H. de Almeida, J. Power Sources 117 (2003) 179.
[6] R.L. Broggi, G.M. de Oliveira, L.L. Barbosa, E.M.J.A. Pallone, I.A. Carlos, J. Appl. Electrochem. 36 (2006) 403.
[7] S. Fletcher, C.S. Halliday, D. Gates, M. Westcott, T. Lwin, G. Nelson, J. Electroanal. Chem. 159 (1983) 267.
[8] A.J. Bard, L.R. Faulkner, Electrochemical Methods: Fundamentals and Applications, John Wiley & Sons, New York, 1980.
[9] T. Berzins, P. Delahay, J. Am. Chem. Soc. 75 (1953) 555.
[10] G. Mamantov, D.L. Manning, J.M. Dale, J. Electroanal. Chem. 9 (1965) 253.
[11] M. Hansen, K. Anderko, Constitution of Binary Alloys, 2nd ed., McGraw Hill, New York, 1958, p. 1106Y.
[12] Y.N. Sadana, Z.H. Zhang, Surf. Coat. Technol. 38 (1989) 299–310.
[13] Joint Committee on Powder Diffraction Standards, JCPDS, in: International Centre for Diffraction Data. Powder Diffraction File, PDF-2, Database Sets 1-49, ICDD, Pennsylvania, 2000 (CDROM).
[14] I. Petersson, E. Ahlberg, J. Electroanal. Chem. 485 (Part I) (2000) 166–177.
[15] I. Petersson, E. Ahlberg, J. Electroanal. Chem. 485 (Part II) (2000) 178–187.